Available online at www.eccomasproceedia.org
Eccomas Proceedia COMPDYN (2023) 3483-3495

ECCOMAS
Proceedia

COMPDYN 2023
9th ECCOMAS Thematic Conference on
Computational Methods in Structural Dynamics and Earthquake Engineering
M. Papadrakakis, M. Fragiadakis (eds.)
Athens, Greece, 12-14 June 2023

SEISMIC COLLAPSE RISK OF A ISOLATED TRANSMISSION TOWER AND A TRANSMISSION LINE SYSTEM IN NORTHERN PORTUGAL

Paiva Fabio M.[1], **Rui C. Barros**[2]

[1] PhD student at Instituto Superior Técnico, Universidade de Lisboa, Lisboa, Portugal
Collaborator of CONSTRUCT R&D Center at FEUP, Porto, Portugal
e-mail: fabiopaiva@tecnico.ulisboa.pt

[2] Jubilled Prof of Structural Engineering
CONSTRUCT, FEUP (Faculdade de Engenharia da Universidade do Porto - Portugal)
email: rcb@fe.up.pt

Abstract

The collapse of the Transmission Line System (TLS) caused by a natural disaster can have serious consequences on the power grid, leading to challenges in the construction or reconstruction of critical infrastructure, reduced quality of community living, compromised disaster response, and potential secondary disasters resulting from interconnected infrastructure. This paper presents a methodology for assessing the seismic collapse risk of a transmission tower (TT) and transmission line system in Northern Portugal. A high-fidelity Finite Element Model of both the isolated tower and the remaining line components (i.e. TLS) was created using the OpenSees framework, and the seismic collapse fragility functions were derived through implementing Incremental Dynamic Analysis. The record-to-record variability of earthquake input is investigated with a set of 40 ground motions records (GMR), using the conditional spectrum for a specific site in Portugal as the target spectrum. The results showed that both the isolated TT and the TLS have acceptable seismic risk of collapse, but the latter system exhibiting a higher seismic collapse risk.

Keywords: Fragility analysis, Three-dimensional modelling, Incremental Dynamic Analysis, Ground motion record selection

ISSN:2623-3347 Published by Eccomas Proceedia.
Peer-review under responsibility of the organizing committee of COMPDYN 2023.
doi: 10.7712/120123.10654.21430

1 INTRODUCTION

Transmission lines system (TLS), or overhead power-lines, is a critical lifeline in modern societies. The electrical grid enables developed countries to sustain high standards of living; however, the risk of local line faults resulting in large-area power outages exists and is growing [1]. Transmission line collapse during a natural disaster may induce cascade failure, which could affect tremendously the local/global economy, and society lifestyle [2]. Seismic waves can transfer an excessive amount of energy in the TLS, which can lead to critical limit states being exceeded, potentially causing local member failures or even the collapse of the transmission tower in the worst-case scenario. However, other earthquake-induced hazards such as ground failure or soil liquefaction are often the primary cause of such collapses, as noted in studies by [3,4].

Assessing the ultimate seismic capacity of the TLS, which is a complex and large-scale electrical and mechanical system, is considered to be one of the most challenging tasks for analysts. To assist in the effort, a high fidelity numerical model of the isolated TT and TLS (three towers and four spans) case study were developed in OpenSees [5]. The isolated TT acts as a baseline for the subsequent TLS (a segment). The main TT has received considerable attention, as the numerical model can capture different member failures modes (yielding, buckling and post-buckling), gusset-plate flexural resistance, in addition to specific lattice tower characteristics joint effects as bolt slippage, joint eccentricities and semi-rigid behaviour at leg-diagonal connection. The IDA is a well-known approach for evaluating the overall collapse condition of a structure and is part of the methodology for generating the collapse fragility function (FF) [6]. To achieve the prior goal, a set of forty multi-component (with two horizontal components) properly selected ground motion records (GMR), based on the conditional spectrum (CS) is employed. The mean annual frequency of collapse (more details in [7]) may be calculated by performing the convolution of the collapse FF and the derivative of the hazard curve (a product of a probabilistic seismic hazard analysis). This allows the analysist to compare with acceptable risk (i.e. empirical approach or code based reliability index) in the TT industry [4].

2 TRANSMISSION LINE DESCRIPTION AND MODELLING ASPECTS

Seismic risk analysis requires a realistic and practical modelling approach that can incorporate various aspects such as tower member/joint ultimate behaviour, tower-line structural coupling and account demand and capacity uncertainties at several stages in the evaluation of the TLS collapse process. This section includes a summary of the TLS case study as well as a concise discussion of the modelling approach that was employed.

2.1 Transmission Line System description

The main TT under investigation is a component of an Overhead High Voltage Line, specifically the Sub-transmission 60 kV Line from EDP, Distribuição (Energias de Portugal). The power line's general layout is illustrated in Fig. 1a), and it “begins” (i.e. main segment represented in figure) in tower 1 and finishes in tower 10, with two significant angle line deviations (i.e. at tower 4 and 6). The TLS case study spans (i.e. segment) are also depicted in the same figure (dashed polygon). As shown in Fig. 1.b), tower 4 (a type F165CD in the operator terminology) was chosen as the critical component for the site-specific risk analysis. Furthermore, because of the substantial horizontal line angle deviation, this TT can be classified as a strain tower type (also known as tension towers in some works) [8].

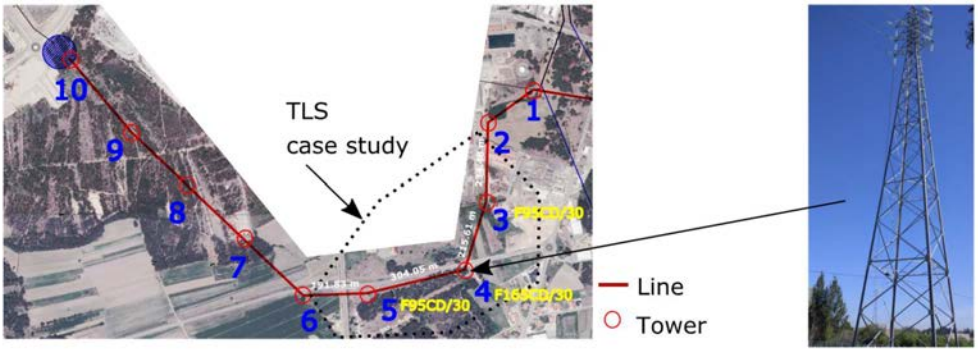

Figure. 1: a) 60 KV Overhead Power-line; b) Tower 4 –F165/CD Strain Tower

The TLS case study consists of four spans of transmission lines (line segment between tower 2 to 6), which are 234.48 m, 215.61 m, 304.05 and 191.83 m, respectively. Additionally, it consists of three towers (38.8-m height) designated as Towers 3 (F95CD/30), Tower 4 (165CD/30) and Tower 5 (F95CD/30) shown in Fig. 2. Despite the fact that tower 4 is less flexible than the adjacent towers, it has a substantial line angle deviation, a line condition that has received less attention.

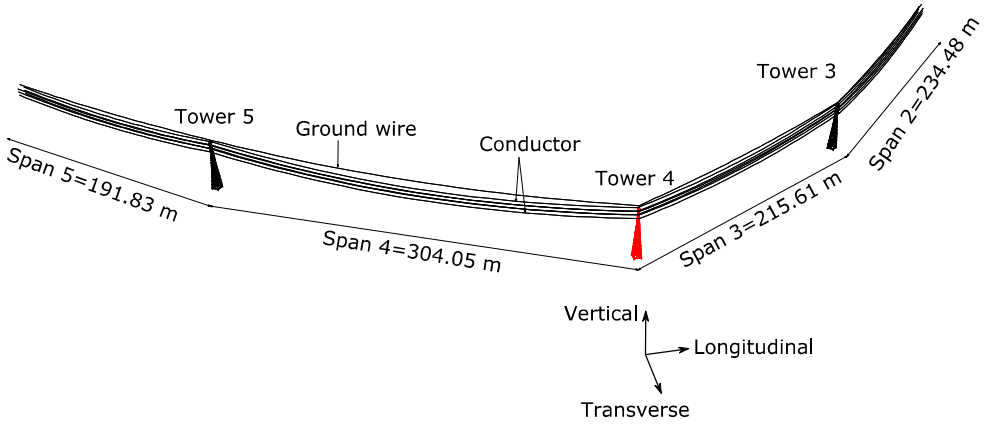

Figure. 2: 3D sketch of the TLS case study

The model's X, Y, and Z axes correspond to the transverse, longitudinal, and vertical directions of the transmission tower-line system, respectively. The line spans are variable, as indicated in the figure. Several significant deviations occur along the power line's path in this segment. The maximum line angle deviation, corresponds to $\Delta = 59.19°$. The overhead power line is supported on three cross-arms, each carrying two conductors (i.e. a double vertical three-phase electric circuit), while the top of the tower is reserved for the ground/shield wire (also known as earth wire).

A recent article by the authors [9] offers an in - depth description of the main TT 4 (cross-sections, main geometry, joint details, material characteristics), which is excluded in this work for brevity. In summary, the lattice tower is made up of steel angles from the S275 class.

For the transmission lines, the conductor (type: ASCR 325 (Bear)) is supported by the top, middle and bottom cross arms, while the ground wire (type: OPGW-AA/ACS/ST 157/60) hang from the top of the lattice tower. Strain insulators (U100 BLP) in toughened

glass L=1.2 m attach the conductor to the TT. Further information about the conductor lines and ground wires is presented in Table 1.

Description	Conductor	Ground wire	Insulator
Designation	ASCR 325	OPGW-AA/ACS/ST 157/60	U100 BLP
Outside Diameter (mm)	23,45	19,60	-
Modulus of Elasticity (GPa)	79,5	84,5	76,5
Cross-sectional area (mm^2)	325	219,66	-
Mass per unit length (kg/km)	1260	868	30 (total mass)
Nominal breaking load (kN)	109,38	112,6	100

Table 1. Mechanical properties of conductor, ground wire and insulator

2.2 A high fidelity Transmission tower numerical model

It is widely acknowledged that the inclusion the full TLS (for example, from tower 1 to tower 10) in the computer model is impracticable and computationally costly. Furthermore, because the coupling action between a tower and a line is confined to a certain extension (usually two-three spans is ideal) from a specific TT, only a sub-system consisting of four transmission line spans and three supporting TT was considered in this study. This TLS dimension is expected to provide sufficient accuracy at an acceptable computation cost.

Typical modelling strategies (e.g., linear analysis of 3D truss models) have major limitations in replicating TT's complex nonlinear behaviour [10]. Damage assessment close to the system ultimate capacity frequently involves the application of algorithms to track the deterioration process throughout the TT brace components (i.e. yielding, buckling, and post-buckling) as well as other nonlinear effects at the joint. Regardless of the fact that the TT should have sufficient strength, stiffness, and ductility to endure large earthquakes events, earlier research has shown a brittle collapse mechanism [11]. When analysing such a complex system, a number of assumptions are made, each of which may have a different influence on seismic capacity assessment and subsequent risk analysis. Examples include component input of the seismic action, numerical models capabilities and neglecting aspect as: ground motion spatial variability effects, material spatial variability in the TT (member and bolts), fabrication errors and improper detailing [12].

In OpenSees, a Fiber-FEM modeling approach was used to mimic the behaviour of steel TT 4 to the collapse state ([13]; [14]; [15]). Member buckling, gusset plate yielding, and joint effects (e.g. slippage, eccentricities and semi-rigid behaviour) may all be simulated with developed numerical model. Paiva and Barros [9] provide detailed information about the development of the TT 4 numerical model in OpenSees.

2.3. Other TLS components

Despite the focus on the high-fidelity TT 4, the remaining transmission line components were modelled to evaluate their impact on the overall risk. This featured two adjacent towers (as simplified elastic models) to the main TT 4, conductors and wire shields, resulting in a system with three towers and four spans. To represent the curved geometry of cables (considered parabolic for small curvatures), a sequence of straight elastic beam-column elements with

a sag equal to 5% of the span is utilized (assumed at serviceability conditions) [16]. Each transmission line was modelled with 30 elastic beam-column. An overview of OpenSees TLS numerical model is given in Fig. 3.

Figure. 3 –Overview of OpenSees TLS numerical model

The remote ends spans of the TLS, were controlled at the relevant heights with zero-length elements in the longitudinal direction and restrained from translational motion in the other directions. These elements were utilized to simulate the tensile restraints imposed by the remaining TT placed beyond the virtual system's two ends. The zero-length element longitudinal stiffness was first computed using equation (35) in [17], and then calibrated to meet the experimental data (identification of TLS fundamental vibration modes in the horizontal directions) [18]. The final remote longitudinal spring stiffness of span 5 (extreme left span) and span 2 (extreme right span), were determined as 50.4 kN/m and 39.78 kN/m, respectively.

2.4. Other modelling considerations

The mass of the TTs has been approximated as lumped at the main joints (leg-braces). This only occurred on TT lowest sections, with the remaining tower having a more realistic distribution. The mass densities of the transmission line materials and the line cross-section were utilized to define the line mass (e.g. kg/km), which was then assigned to the line nodes. In addition, the mass of the strain insulator was added as lumped mass to cross-arm tips.

The damping model in the Rayleigh form, proportional to the mass and to the initial stiffness matrix ($C=\alpha M+\beta K0$) is adopted [19]. The parameters α and β are grounded on the fundamental frequency f_1 and a second frequency equal to $5*f_1$. The f_1 frequency corresponds to the fundamental frequency of each subsystem (i.e. towers or transmission lines). Damping ratios of 5% and 1% were applied in the supporting steel towers and transmission lines, respectively. The dynamic properties of the transmission tower-line system of the OpenSees model are evaluated in terms of natural frequencies and compared to experimental data [18]. The first flexural vibration mode in the transversal direction was 2.47 Hz, while in the longitudinal direction the value was 2.23 Hz. As can be noted, the frequencies of the TLS were observed to be lower than those of the isolated TT (3.3 Hz).

3 SITE HAZARD AND SELECTION OF GROUND MOTION RECORDS UNDER SELEQ APPLICATION

An optimal IM is crucial in the seismic risk evaluation process [20]. TT seismic fragility studies have recognized the significance of using the spectral acceleration $S_a(T_1,5\%)$ at the fundamental period of the structure as having significant properties of an optimal IM [21]. Typically, the Sa reveals adequate properties for first dominated structures, which exhibit a brittle

or poor ductility behaviour [22]. With this in account, S_{agm}, as defined by earth scientists (geometric mean of spectral acceleration of two orthogonal horizontal components), is used as the IM in the current study [23].

3.1. Site hazard characterization

PSHA was carried out at the site of interest with the use of the open source program OpenQuake [24]. This was made possible with SelEQ software [25], and the seismic hazard models delivered in the SHARE project. In addition to the model supplied by the SHARE project, other hazards sources for the Portuguese territory were incorporated into PSHA [26].

At the TLS location (i.e. TT4), the site-specific median hazard curve is shown in terms of the IM= $S_{agm}(T_{eq},5\%)$ in Figure 4. The ground type C was assumed at the site location. All computations assume a 5% damping and are thus omitted. The IM=S_{agm}= $\sqrt{S_{ax}(T_{eq}) \cdot S_{ay}(T_{eq})}$ is denoted as $S_a(T_{eq},5\%)$ in this work, where S_{ax} is the spectral acceleration of x horizontal component and S_{ay} is the spectral acceleration of y horizontal component. The IM adopted is computed at the equivalent period T_{eq} for the TLS and T_{eq}=T_1 for the isolated TT. This equivalent period is defined as the geometric mean of the two periods of vibration, T_{1x} and T_{1y}, where T_{1x} is fundamental period in the x direction (transversal direction in this work), and T_{1y} fundamental period in the y direction (longitudinal direction), resulting in $T_{eq} = \sqrt{T_{1x} \cdot T_{1y}}$ as the option selected in this work [23]. For TLS this value is equal to T_{eq}=0.42 s and for isolated tower corresponds to T_1=0.30s

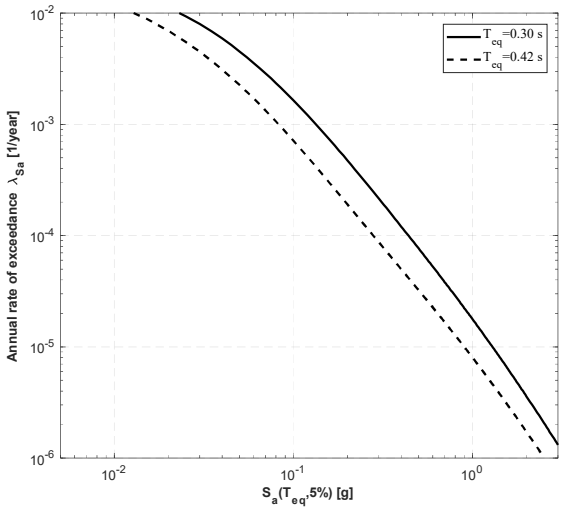

Figure. 4 - Seismic Hazard curve (median) for Teq= 0.42 and 0.30 s for a soil type C

3.2. Selection of Ground motion records

The importance of the spectral shape has been noted by several researchers, as a critical element improve the quality of ground motion set [7], [27]. Conditional Spectrum (CS) is one of the most important methods for selecting GMR developed in the last decades [25]. Unlike traditional code-based spectrum or Uniform Hazard Spectrum (UHS), a CS-based target spectrum selection explicitly considers for spectral shape.

The CS-based record selection comprises the use of SelEQ framework to compute the target CS for the case study site of interest (in the north of Portugal). The CS at the site was computed using a hazard level associated with a 475-year mean return period. The preliminary seismological criteria (e.g. magnitudes, epicentre distance and ground type) were established using PSHA disaggregation data. The record selection method consisted of minimizing the determined record set's mean and variance mismatches with regard to the CS target mean and standard deviation [25]. The set of forty GMR selected and scaled according to the aforementioned criteria is shown in Fig. 5-6. The set of records' mean and variance response spectrum closely follows the target spectrum. The response spectra of the GMR studied in this paper demonstrate the inherent uncertainty that they entail.

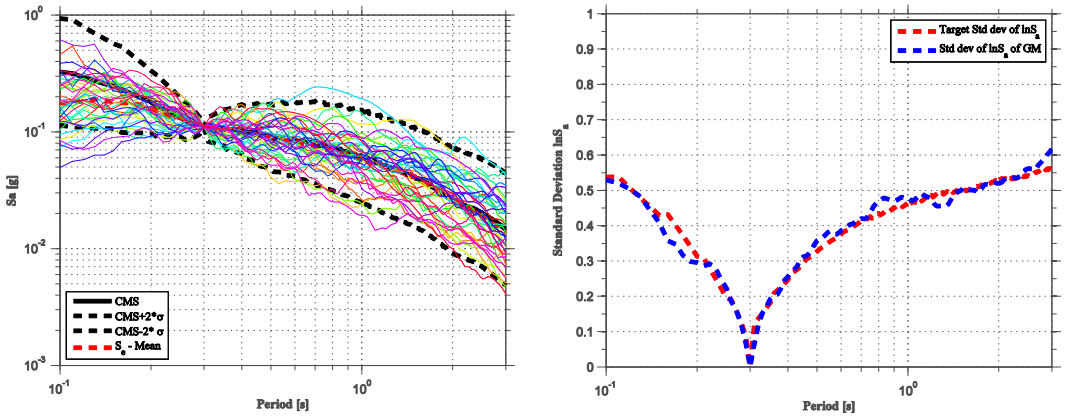

a) b)

Figure. 5 - Application of SelEQ to a CS-based record selection case, Isolated TT (T_1=0.30s), 10% in 50y a) mean; b) variance

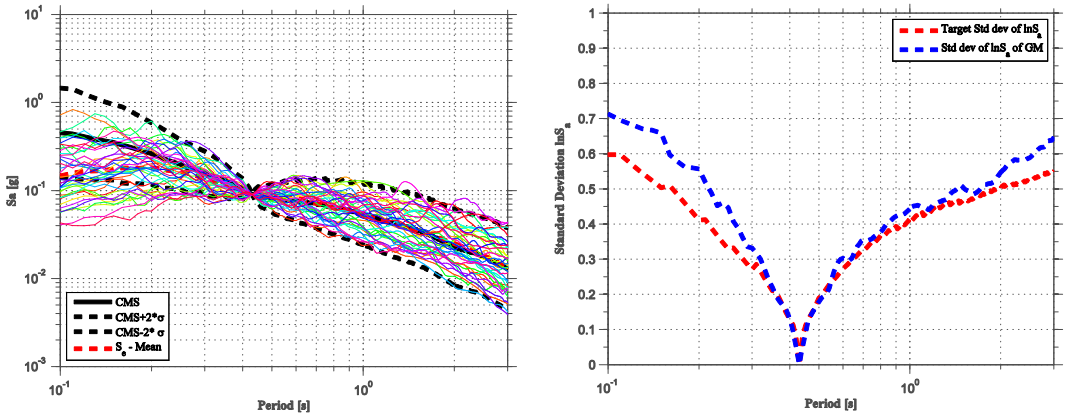

a) b)

Figure. 6 - Application of SelEQ to a CS-based record selection case, TLS (T_{eq}=0.42s), 10% in 50y a) mean; b) variance

The two horizontal components of each GMR are applied to the numerical model in both the transversal and longitudinal directions.

4 TT/TLS SEISMIC COLLAPSE RISK

The results here presented constitute an updated more detailed and justified version, of those presented earlier [28]-[29].

IDA will serve as the foundation of the applied seismic collapse risk framework in this study. Using the IDA approach, the GMR are scaled up (IM=$S_a(T_{eq},5\%)$) until collapse is achieved. Structural collapse is defined as a non-numerical convergence.

4.1. Seismic Collapse Fragility analysis of isolated TT and TLS

The plot of IM versus maximum Inter Section Drift Ratio (ISDR) ([11] provides further information) is calculated for each GMR, hence describing the evolution of the IDA curves. Figure 7 shows the IDA curves of the isolated TT for the ISDR. It is possible to verify that some degree of nonlinearity exists in multiple IDA curves, despite the fact that it does not appear to be particularly significant. This clearly suggest a fragile failure mode developed by the TT.

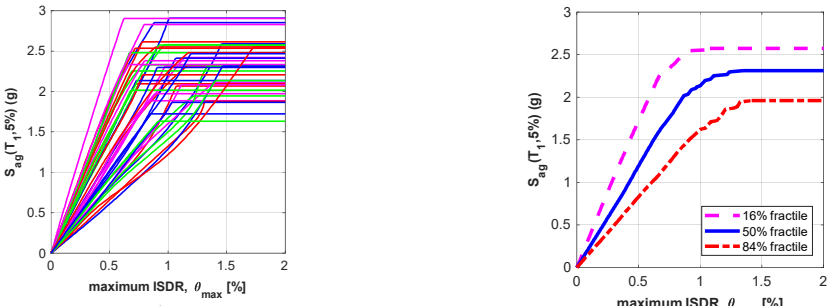

a) b)

Figure. 7 - IDA curves of isolated TT in terms of $S_{ag}(T_1)$ and the maximum ISDR a) all IDA curves b) IDA curves summarized in fractiles

As can be observed in Fig. 8, the IDA curve's initial behaviour for TLS is somewhat unexpected; however, the explanation is connected to the influence of gravity action on the transmission lines (i.e. unbalance tension imposed to the TT). Following that, the curve exhibits a linear trend in nearly every GMR until it reaches the ultimate state. This suggests that the TT4 has developed a brittle failure mode.

The S_a capacities range within the 0.56g to 1.94g. It is possible to observe ISDR capacities associated with the collapse state in the 0.25-0.95% range.

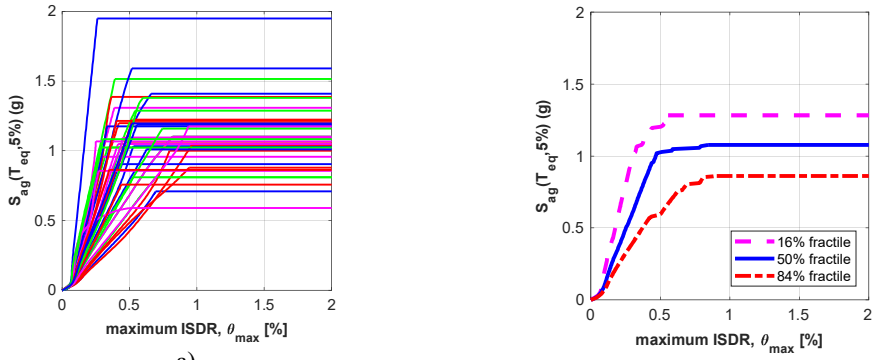

a) b)

Figure. 8 - IDA curves of TLS in terms of $S_a(T_{eq})$ and the maximum ISDR a) all IDA curves b) IDA curves summarized in fractiles

The collapse FF of the isolated TT and TLS is plotted in Fig. 9. The resulting function (i.e. lognormal distribution [30]) of the isolated TT has a median capacity of $\widehat{\boldsymbol{\theta}_r}$=2.28g and dispersion of $\widehat{\boldsymbol{\beta}_r}$=0.139. In the case of the TLS the generated FF has a median capacity of $\widehat{\boldsymbol{\theta}_r}$=1.08g and a dispersion of $\widehat{\boldsymbol{\beta}_r}$=0.226 .

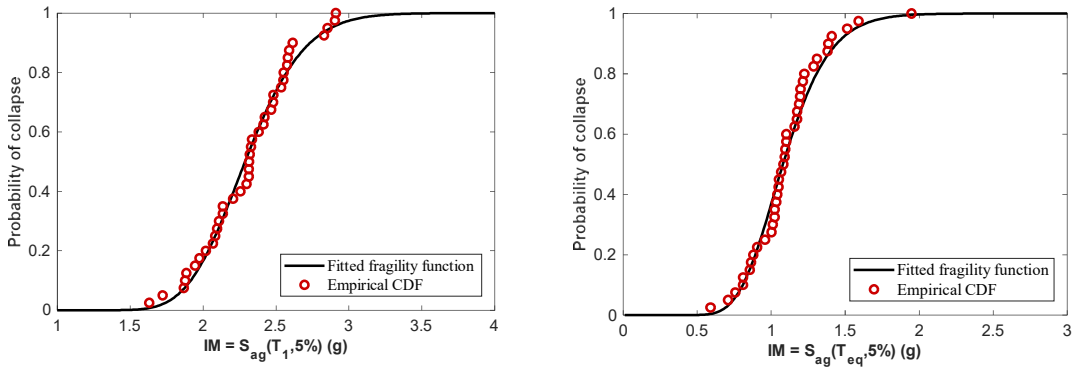

a) Isolated TT b) TLS

Fig. 6 - Collapse fragility function of the TT and TLS under multi-component ground motion records

The TLS collapse probability under a very rare earthquake scenario ($S_a(T_{eq})$=0.64g, mean return period of 2475 years) is close to 1%. This satisfies the 10 % collapse probability limit proposed in FEMA – P695 [31] under the Maximum Credible Earthquake (MCE). The isolated TT's collapse probability under a Maximum Credible Earthquake scenario ($S_a(T_1)$ =0.90g) is near zero, satisfying the guideline collapse probability limit by a large margin.

When an extremely rare earthquake scenario (exceedance probability of 1%/ in 50y) is considered, the probability of collapse approaches 0.002% for the isolated TT and 24 % for the TLS. The last scenario in the TLS, because of its magnitude, depicts a situation that may necessitate some attention for important structures. The collapse margin ratio (CMR) is another metric used to assess structural collapse resistance capacity [31]. In the case of the isolated TT the CMR translates to a value of around 2.5, indicating a moderate/high CMR, implying that the current TT is not susceptible to collapse. For the TLS, a CMR of about 1.69 suggests a low to moderate vulnerability to collapse.

4.2. Seismic Risk Analysis

The annual frequency of collapse $\boldsymbol{\lambda_c}$ is main metric for assessing risk of collapse of the TT in this study. The $\boldsymbol{\lambda_c}$ IM-based approach (more details in [7] and [30]), and involves integrating the structure specific seismic FF with the ground motion hazard curve. Because these two ingredients have previously been identified, the computation is accomplished by numerical integration [7]. The predicted annual frequency of collapse and other equivalent risk metrics (i.e. probability of collapse in 50y and reliability index in 1y or 50 y) for the two system under analysis are shown in Table 2.

Model	$\hat{\lambda}_c$ (1/year)	$\hat{P}$c,50y(%)	$\hat{\beta}$1y	$\hat{\beta}$50y
Isolated TT	2.41*10^{-6}	0.012%	4.57	3.67
TLS	6.91*10-6	0.034%	4.34	3.39

Table 2. Summary of the seismic collapse risk analysis in equivalent metrics

Additional efforts have been made to characterize the λ_c estimation uncertainty, owing to the response variability from record to record ground motion [32]. Since a point estimate of the annual frequency, defined as the mean, has already been obtained, the aim now is to evaluate the expected value and variance of the risk estimator. To better characterize this risk metric, the bootstrap method (random sampling with replacement) is used [33]. This calculation employs 1000 parametric simulation extractions, under the assumption that FF has a parametric representation (i.e. lognormal model), and the main statistics generated are included in table 3.

Model	$E[\hat{\lambda}_c]$ (1/year)	$Var[\hat{\lambda}_c]$	$C.o.v[\hat{\lambda}_c]$
Isolated TT- Parametric Bootstrap	$2.39*10^{-6}$	$2.14*10^{-14}$	6%
TLS-Parametric Bootstrap	6.95*10-6	3.86*10-14	9%

Table 3. Quantification of collapse seismic risk uncertainty due to record to record variability

With this information, the annual frequency of collapse associated with 2 standard deviations, for example, yields λ_c= $2.09*10^{-6}$- $2.68*10^{-6}$ for the isolated TT and λ_c= $5.71*10^{-6}$ - $8.19*10^{-6}$ for the TLS. This translates to a roughly threefold increase in the likelihood of collapse of the TLS compared to the isolated TT. The determined probability of failure for TT is significantly lower (almost a magnitude lower) than the suggested acceptable values in the literature, such as Kempner [4], which "proposed" an acceptable target of 0.15 % in 50 y (risk category III according to the American code practice). This demonstrates that the both examples examined have a more than satisfactory seismic risk of collapse.

CONCLUSIONS

In the OpenSees framework a complex TLS numerical model was built. In addition to taking into account critical system components (e.g. TTs and transmission lines), the emphasis was on a particular high-fidelity TT model. For an accurate collapse evaluation, many nonlinear phenomena were accounted for in the study. The isolated TT model was also compared throughout all the study to the TLS, as a mean to address the effect of tower-line coupling in the seismic response. The IDA approach forms the backbone of the collapse seismic fragility study. In order to undertake a robust analysis of the system's ultimate dynamic behaviour, forty GMR were chosen based on the CS target spectrum at the site of interest. This, together with PSHA and one of its outputs, the hazard curve, enabled the determination of the annual frequency of collapse (λ_c) of the TT (with and without the line effects).

Aside from the collapse seismic fragility function, the λ_c was another notable contribution of this risk study. Its relevance may assist transmission line operators to manage the seismic risk revealed by their infrastructures more effectively. According to the conclusions of this study, the TLS has a minimal risk of collapse (a mean of 0.034% in 50 years). This was found to be three times larger than the seismic collapse risk displayed by isolated TT. In both situations, the seismic collapse risk achieved was considered acceptable.

ACKNOWLEDGEMENTS

The first author acknowledges the financial support from Fundação para a Ciência e a Tecnologia (FCT, Ministério da Educação e Ciência, Portugal) through the scholarship PD/BD/127799/2016 - FCT Doctoral Program: Analysis and Mitigation of Risks in Infrastructures (INFRARISK).

This work is also supervised by the second author within the scope of the Project "SD Poles - Steel and Dampers for Poles" with reference POCI-01-0247-FEDER-039865, co‐financed by European Regional Development Fund (ERDF) through the Operational Programme for Competitiveness and Internationalization (COMPETE 2020) under the PORTUGAL 2020. Besides, this work is also integrated in the general R&D activities of the CONSTRUCT Institute on Structures and Constructions (Instituto de I&D em Estruturas e Construções), financially supported by Base Funding UIDB/04708/2020 through national funds of FCT/MCTES (PIDDAC).

REFERENCES

[1] Organization for Security and Co-operation in Europe (OSCE). *Protecting Electricity Networks from Natural Hazards*, Vienna, Austria, 2016.

[2] E. Ghannoum. A Rational Approach to Structural Design of Transmission Line. *IEEE Transactions on Power Apparatus and Systems*, **PAS-100** (7): 3506–3512, 1981. https://doi.org/10.1109/TPAS.1981.316694

[3] G. Karagiannis, C. Stamatios, E. Krausmann, Z.I. Turksever. *Power Grid Recovery after Natural Hazard Impact. JRC Science for policy Report*, Luxembourg, 2017. https://doi.org/10.2760/87402

[4] L. Kempner. Question: What Is an Acceptable Target Reliability for High-Voltage Transmission Lines? *In Electrical Transmission and Substation Structures 2018*: Dedicated to Strengthening Our Critical Infrastructure - Proceedings of the 2018 Electrical Transmission and Substation Structures Conference, 281–289. https://doi.org/10.1061/9780784481837.026

[5] S. Mazzoni, F. Mckenna, M.H. Scott, G.L. Fenves. *Open System for Earthquake Engineering Simulation, User Command-Language Manual (Report NEES Grid-TR 2004–21*). Pacific Earthquake Engineering Research (PEER) Center, 2006.

[6] D. Vamvatsikos, C.A. Cornell. Incremental Dynamic Analysis. *Earthquake Engineering and Structural Dynamics*, 31 (3): 491–514, 2002. https://doi.org/10.1193/1.1737737.

[7] L. Eads. *Seismic Collapse Risk Assessment of Buildings: Effects of Intensity Measure Selection and Computational Approach*. Ph.D. Thesis, Stanford University, USA, 2013.

[8] F. Kiessling, P. Nefzger, J.F. Nolasco, U. Kaintzyk. *Overhead Power Lines - Planning, Design and Construction*. Heidelberg: Springer-Verlag, Berlin, Germany, 2003.

[9] F. Paiva, R.C. Barros. Capacity Assessment of a High-Voltage Lattice Tower Under Different Loading Patterns. *7th International Conference on Integrity-Reliability-Failure (IRF2020)*, Funchal, Portugal, 2020.

[10] E. Tapia-Hernández, S. Ibarra-González , D. De-León-Escobedo. Collapse Mechanisms of Power Towers under Wind Loading. *Structure and Infrastructure Engineering,* **13** (6): 766–82, 2017 https://doi.org/10.1080/15732479.2016.1190765.

[11] L. Tian, R. Ma, Q. Bing. Influence of Different Criteria for Selecting Ground Motions Compatible with IEEE 693 Required Response Spectrum on Seismic Performance Assessment of Electricity Transmission Towers. *Engineering Structures*, **144**: 337–350, 2018. https://doi.org/10.1061/(ASCE)ST.1943-541X.0002000.

[12] R.N. Prasad, G.M. Samuel Knight, S.J. Mohan, N. Lakshmanan. Studies on Failure of Transmission Line Towers in Testing. *Engineering Structures*, **35**: 55–70, 2012. https://doi.org/10.1016/j.engstruct.2011.10.017.

[13] P. Uriz P, S.A. Mahin. *Toward Earthquake-Resistant Design of Concentrically Braced Steel-Frame Structures* - PEER 2008/08 Report. Pacific Earthquake Engineering Research Center, Berkeley, California, USA, 2008.

[14] E. Karamanci, D.G. Lignos. Computational Approach for Collapse Assessment of Concentrically Braced Frames in Seismic Regions. *Journal of Structural Engineering* 140 (8): A4014019, 2014. https://doi.org/10.1061/(ASCE)ST.1943-541X.0001011.

[15] A. Aguero, C. Izvernari, R. Tremblay. Modeling of the Seismic Response of Concentrically Braced Steel Frames Using the OpenSees Analyis Environment. *Int. J. Adv. Steel Constr.* 2: 33, 2006.

[16] R. C. Battista, R.S. Rodrigues, M.S. Pfeil. Dynamic behavior and stability of transmission line towers under wind forces. *Journal of Wind Engineering and Industrial Aerodynamics* ,91 (8),1051-1067, 2003.

[17] Y.M. Desai, P. Yu, M. Popplewell, A.H. Shah A.H. Finite Element Modelling of Transmission Line Galloping. *Computers & Structures* **57** (3): 407–420, 1995. https://doi.org/10.1016/0045-7949(94)00630-L.

[18] F. Paiva F, R.C. Barros, L. Guerreiro. Dynamic Structural Health Monitoring of a Transmission Tower using Interferometric radar. *6th International Conference on Integrity-Reliability-Failure (IRF2018)*, Lisbon, Portugal, 2018.

[19] A. Hardyniec, F. Charney. An Investigation into the Effects of Damping and Nonlinear Geometry Models in Earthquake Engineering Analysis. *Earthquake Engineering & Structural Dynamics* **44** (July): 2695–2715, 2015. https://doi.org/10.1002/eqe

[20] S. Ghosh, S. Ghosh, S. Chakraborty. Seismic Fragility Analysis in the Probabilistic Performance-Based Earthquake Engineering Framework: An Overview." *International Journal of Advances in Engineering Sciences and Applied Mathematics*, no. December: **14**, 2017. https://doi.org/10.1007/s12572-017-0200-y.

[21] H. Pan, T. Li, F. Xing, L. Hongnan. Sensitivities of the Seismic Response and Fragility Estimate of a Transmission Tower to Structural and Ground Motion Uncertainties. *Journal of Constructional Steel Research* **167**: 105941, 2020. https://doi.org/10.1016/j.jcsr.2020.105941.

[22] D. Vamvatsikos. Analytic Fragility and Limit States [P(EDP|IM)]: Nonlinear Dynamic Procedures. In *Encyclopedia of Earthquake Engineering*, 15, 2015. https://doi.org/https://doi.org/10.1007/978-3-642-35344-4_247.

[23] J.W. Baker, C.A. Cornell. Which Spectral Acceleration Are You Using? *Earthquake Spectra*, **22** (2): 293–312, 2006. https://doi.org/10.1193/1.2191540.

[24] M. Pagani, F.Monelli, G. Weatherill, L. Danciu, H. Crowley, V. Silva, P. Henshaw, et al.. OpenQuake Engine: An Open Hazard (and Risk) Software for the Global Earthquake Model. *Seismological Research Letters* **85** (3): 692–702, 2014. https://doi.org/10.1785/0220130087.

[25] L. Macedo, J.M. Castro. SelEQ: An Advanced Ground Motion Record Selection and Scaling Framework. *Advances in Engineering Software*, **0**: 1–16, 2017. https://doi.org/10.1016/j.advengsoft.2017.05.005.

[26] S.P. Vilanova, J.F.B.D. Fonseca. Probabilistic Seismic-Hazard Assessment for Portugal. *Bulletin of the Seismological Society of America* **97** (5): 1702–1717, 2007. https://doi.org/10.1785/0120050198.

[27] J.W. Baker, C.A. Cornell. A Vector-Valued Ground Motion Intensity Measure Consisting of Spectral Acceleration and Epsilon. *Earthquake Engineering and Structural Dynamics*, **34** (10): 1193–1217, 2005. https://doi.org/10.1002/eqe.474.

[28] F. Paiva, R.C. Barros. Seismic Collapse Risk of a Transmission Tower. Contribution 8926 at the 3rd European Conference on Earthquake Engineering & Seismology, Bucharest, Romania, 2022.

[29] F. Paiva, R.C. Barros. Seismic Collapse Risk of a Transmission Line System. Contribution 0754 at the 3rd European Conference on Earthquake Engineering & Seismology, Bucharest, Romania, 2022.

[30] J.W. Baker. Efficient Analytical Fragility Function Fitting Using Dynamic Structural Analysis. *Earthquake Spectra*, **31** (1): 579–599, 2015. https://doi.org/10.1193/021113EQS025M

[31] Federal Emergency Management Agency (FEMA). *Quantification of Building Seismic Performance Factors - FEMA P695*, Washington, DC, USA, 2009.

[32] I. Iervolino. Assessing Uncertainty in Estimation of Seismic Response for PBEE. *Earthquake Engineering & Structural Dynamics*, **13**, 2017. https://doi.org/10.1002/eqe.2883.

[33] R. Baraschino, G. Baltzopoulos, I. Iervolino I. R2R-EU: Software for Fragility Fitting and Evaluation of Estimation Uncertainty in Seismic Risk Analysis. *Soil Dynamics and Earthquake Engineering,* **132** (February): 106093, 2020. https://doi.org/10.1016/j.soildyn.2020.106093